PRELIMINARY RESULTS OF FISHERIES INVESTIGATION ASSOCIATED WITH SKYLAB-3

K. Savastano, E. Pastula, Jr., and G. Woods

National Marine Fisheries Service
Bay St. Louis, Mississippi

K. Faller

Earth Resources Laboratory
National Aeronautics and Space Administration
Bay St. Louis, Mississippi

April 15, 1974

Skylab Experiment No. 240
NASA Contract No. T-8217B

PRELIMINARY RESULTS OF FISHERIES INVESTIGATION ASSOCIATED WITH SKYLAB-3

K. Savastano, E. Pastula, Jr., and G. Woods

National Marine Fisheries Service
Bay St. Louis, Mississippi

K. Faller

Earth Resources Laboratory
National Aeronautics and Space Administration
Bay St. Louis, Mississippi

ABSTRACT

The purpose of the 15-month investigation now in the analysis phase is to establish the feasibility of utilizing remotely sensed data acquired from aircraft and satellite platforms to provide information concerning the distribution and abundance of oceanic gamefish. Data from the test area, jointly acquired by private and professional fishermen and NASA and NOAA/NMFS elements, in the northeastern Gulf of Mexico has made possible the identification of fisheries significant environmental parameters for white marlin. Predictive models based on catch data and surface truth information have been developed and have demonstrated potential for reducing search significantly by identifying areas which have a high probability of being productive. Three of the parameters utilized by the model, chlorophyll-a, sea surface temperature and turbidity have been inferred from aircraft sensor data. Cloud cover and delayed receipt have inhibited the use of Skylab data. The first step toward establishing the feasibility of utilizing remotely sensed data to assess and monitor the distribution of oceanic gamefish has been taken with the successful identification of fisheries significant oceanographic parameters and the demonstration of the capability of measuring most of these parameters remotely.

INTRODUCTION

A 15-month investigation of oceanic gamefish was initiated in April 1973, with the field operations phase conducted on August 4 and 5, 1973, in the northeastern Gulf of Mexico. This joint effort by private and professional fishermen and NASA and NOAA/NMFS elements was undertaken to acquire fishery and oceanographic data in association with near simultaneously acquired Skylab-3 and aircraft remotely sensed environmental data. Currently the investigation is well advanced into the postmission or analysis phase with completion scheduled for June 1974. This paper presents a summary of the results to date of the investigation. An earlier paper described the field operations of August 4 and 5, 1973 (Woods and Cook, 1973).

The primary objective of the investigation is to establish the feasibility of utilizing remotely sensed data acquired from aircraft and satellite platforms to assess and monitor the distribution of oceanic gamefish. This is being explored through a series of correlations among aerospace (satellite/aircraft) imagery, spectrometry, and sea truth information related to the marine environment and the gamefish resource. Available Skylab and aircraft underflight data have been analyzed in conjunction with sea truth oceanographic measurements and oceanic gamefish distribution data acquired during field operations in the test area.

The target resource of the investigation, oceanic gamefish, is construed to include the billfishes, dolphin, wahoo and certain of the tunas for the purpose of this investigation. The gamefish constitute a major source of recreation for an ever increasing number of saltwater anglers. In addition to the increasing domestic pressure, the resource is being exploited by the Japanese longline fishery and there are indications (Fox, 1971) that the fishing intensity has reached or exceeded that level which would provide a maximum sustainable annual yield. The application of new management techniques may be required in the near future to protect the resource.

TEST AREA

The test area (Figure 1) comprised 18000 square kilometers and was shaped roughly like a triangle, bounded by the coordinates $30^{o}16'$N, $86^{o}51'$W; $29^{o}18'$N, $85^{o}47'$W; and $29^{o}21'$N, $87^{o}56'$W on the north, east and west, respectively. The northern apex lay 14 kilometers south of Santa Rosa Island and the southern serrated edge extended 155 km south of the apex. The sides extending from the northern apex approximated the 55 meters curve along the coast. The northern extremity of the De Soto Canyon lay within the southern portion of the area providing depths in excess of 1600 meters. In order to provide a grid for referencing gamefish catches, the fishing area was divided into 54 squares with 18.3 km (10 nautical miles) to a side. Skylab track 62 approximately bisected the area, extending southeast from Mobile Bay.

The test area is noted for a relative abundance of oceanic gamefish during the summer season. Numerous marinas are located along the coastline. Several gamefishing clubs are headquartered in nearby coastal cities and charterboat gamefishing is a viable industry in the coast economy.

FIELD OPERATIONS AND DATA ACQUISITION

Skylab EREP Imagery

The Skylab Earth Resources Experiment Package (EREP) overpass occurred at approximately 1140 local time on August 5 with 40 to 70 percent scattered cumulus cloud cover below 3000 meters. The sensors activated during the overpass are shown with their respective applications for the project in Table I.

TABLE I. SKYLAB EREP SENSORS ACTIVATED

INSTRUMENT	DESCRIPTION	FOOTPRINT	APPLICATION
S190 A	6 Cameras	161 km. wide	Water Color, Surface Features
S190 B	1 Camera	108 km. wide	Water Color, Surface Features
S191	Infrared Spectrometer	.43 km. wide	Water Color, Sea Surface Temperature
S192	Multispectral Scanner	68 km. wide	Water Color, Sea Surface Temperature
S194	Microwave Radiometer	109 km. wide (half power)	Sea Surface Salinity

Aircraft Imagery

Two aircraft flew data gathering missions in the area on the morning of 5 July. A NASA earth survey aircraft, the NC130B, based in Houston, Texas, flew three flight lines totaling 413 km through the area at 6100 meters altitude. A contract light aircraft flew transects totaling 413 km at 3000 meters altitude. The aircraft sensor coverage is given in Table II.

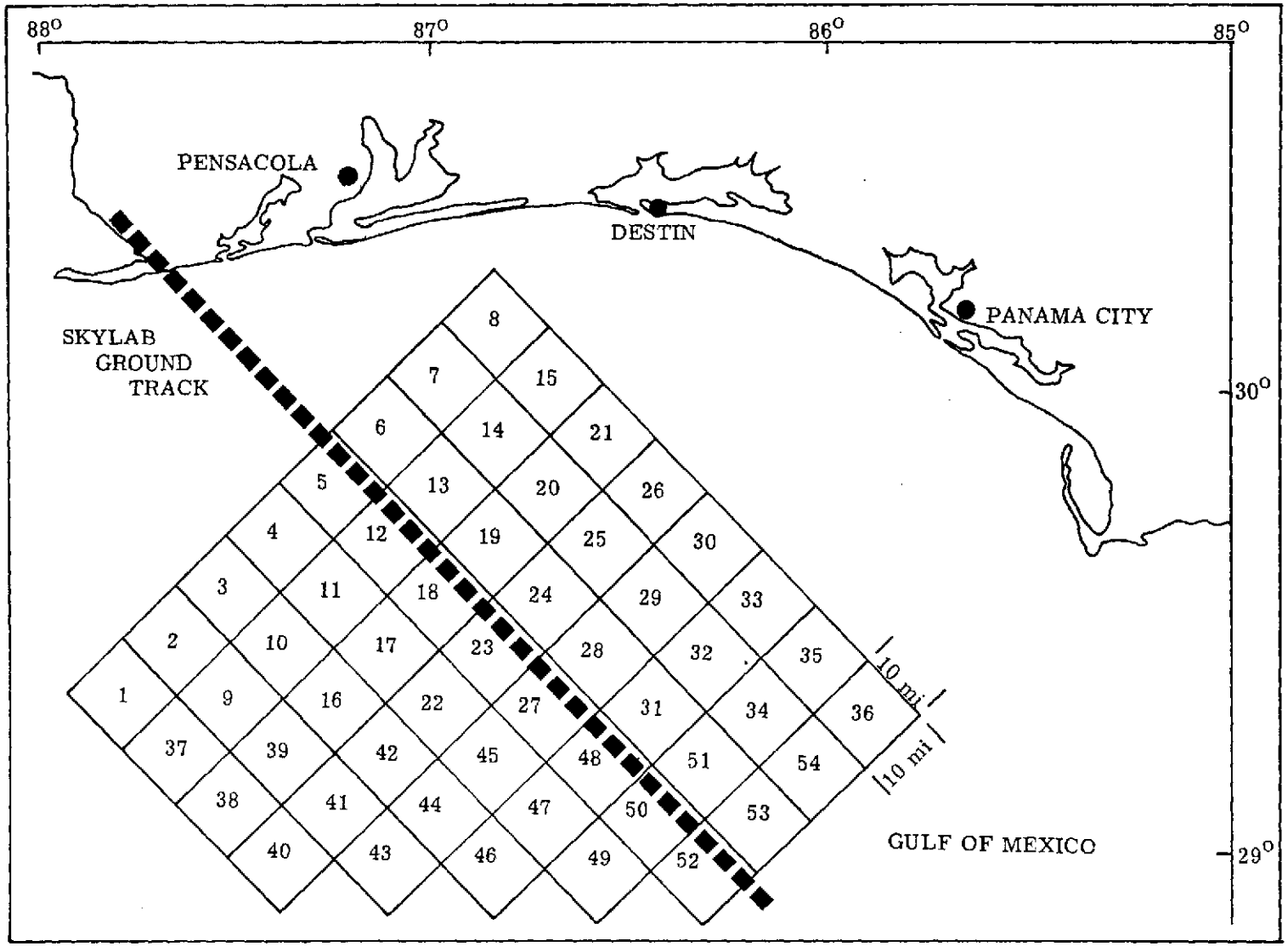

FIGURE 1. TEST AREA WITH FISHING SQUARES

TABLE II. AIRCRAFT SENSOR COVERAGE

INSTRUMENT	DESCRIPTION	FOOTPRINT	USE
NASA NC130B			
MSS	Multispectral Scanner	10.2 km	Sea Surface Temperature , Water Color
RECON IV	Infrared Scanner	7.0 km	Sea Surface Temperature
AMPS	Airborne Multispectral Photographic System	2.3 km	Water Color
RC8	Aerial Camera/Color Photography	9.1 km	Cloud Cover, Water Color, Location of Surface Vessels and Features
I^2S	Multiband Camera	5.3 km	Water Color
PRT 5	Precision Radiation	0.2 km	Water Color
NASA Light Aircraft			
RS-18	Thermal Infrared Scanner	7.3 km	Sea Surface Temperature
K-17	Aerial Camera/Color Photography	4.8 km	Water Color, Surface Features
EL 500	2 Cameras - Color and Color IR	4.2 km	Water Color, Surface Features
PRT 5	Precision Radiation Thermometer	0.1 km	Sea Surface Temperature
E 20-D	Spectrometer	0.1 km	Water Color

Sea Truth Measurements

Data task teams on four Government and five Government-chartered vessels operating out of Orange Beach, Alabama, Destin. Florida, and Panama City, Florida, gathered sea truth environmental data at 48 sampling stations at periodic intervals during daylight hours on August 4 and 5. A total of 140 sets of measurements were taken.

Parameters measured for each set included surface water temperature, air temperature, Secchi disc extinction depth (as measure of turbidity), sea state. wind direction and speed, wet and dry bulb temperature, water depth, atmospheric pressure, visibility, cloud cover and type, and water color. Sea water samples were also taken for laboratory analysis for salinity and chlorophyll-a, -b, and -c. The Forel-Ule color comparator was used to determine water color. Sea surface temperature was obtained by means of a bucket thermometer. In addition, portable salinometers were used on several vessels to obtain in situ salinity and temperature measurements.

In addition to data acquisition by the oceanographic vessels, observers on twelve of the larger gamefishing boats collected sea truth data coincident with their gamefish catches. A total of 75 sets of measurements were taken by the observers on gamefishing boats. Parameters measured were the same as those measured from the oceanographic boats except that chlorophyll samples were not taken. Pyschrometer readings were taken on only a few boats.

Gamefish Data

A committee of representatives from six gamefishing clubs and charterboat associations headquartered in Alabama, Florida, and Louisiana, coordinated the volunteer fishing program to acquire data on the living marine resource. These data were acquired through a Skylab Gamefish Tournament held August 4-5 under the general management of the Pensacola Big Game Fishing Club. Fishing tournament officials restricted competition for trophies to seven offshore gamefish species.

Blue Marlin, Makaira nigricans
White Marlin, Tetrapturus albidus
Sailfish, Istiophorus platypterus
Wahoo, Acanthocybium solanderi
Dolphin, Coryphaena hippurus
Yellowfin Tuna, Thunnus albacares
Bluefin Tuna, Thunnus thynnus

Approximately 325 anglers fished from craft, 20 to 57 feet in length, scattered over the test area. On each boat a gamefish log was kept of all fish raised, hooked, lost and boated. Gamefish samplers collected the logs in the late afternoon at the checkpoints from the returning boats. At the time of submission, each log was reviewed by a gamefish sampler with the respective boat captain for omissions and errors while details still remained fresh in mind. Table III gives a breakdown of the fish catch.

TABLE III. TOURNAMENT FISH CATCH

Fish Species	No. Raised But Not Hooked		No. Hooked		No. Lost		No. Boated	
	4 Aug.	5 Aug.	4 Aug.	5 Aug.	4 Aug.	5 Aug.	4 Aug.	5 Aug.
BILLFISH								
Blue Marlin	5	3	6	5	6	5	0	0
White Marlin	25	19	32	23	9	14	23	9
Sailfish	4	5	10	4	6	3	4	1
Total Each Day	34	27	48	32	21	22	27	10
OTHER GAMEFISH								
Yellowfin Tuna	0	0	0	0	0	0	0	0
Bluefin Tuna	0	0	0	0	0	0	0	0
Dolphin	2	0	32	43	5	5	27	38
Wahoo	4	0	10	6	2	3	8	3
Total Each Day	6	0	42	49	7	8	35	41
ALL TOURNAMENT GAMEFISH								
Total Each Day	40	27	90	81	28	30	62	51
Tournament Totals	67		171		58		113	

DATA ANALYSIS

Approach

The primary objective of the investigation was to establish the feasibility of using satellite and aircraft acquired, remotely sensed data to determine the availability and distribution of oceanic gamefish. Sensor capabilities precluded direct observation of the gamefish and restricted information acquisition to surface or near surface phenomena. Accordingly, an indirect approach was required using intermediate correlations. The resource data and remotely sensed information would be separately related to the sea environment as observed by surface sampling and through the latter relationship to each other. Figure 2 shows the relationship.

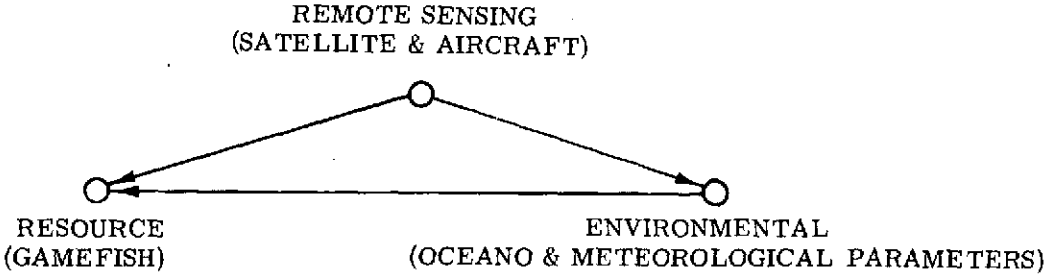

FIGURE 2. ANALYSIS APPROACH

Resource and Environment Relationships

System Concept. The concept employed in the analysis was that oceanic gamefish abundance and distribution can be expressed as a function of the environment, which is similar to that concept expressed in a previous fisheries remote sensing paper (Kemmer et al, 1973). The functional dependence is described in the following algebraic expressions:

$$A_{x,y} = f(E)$$

$$D_{x,y} = f(E)$$

where:

A = number of oceanic gamefish
x, y = fish location coordinates
E = environmental conditions at x, y
D = gamefish distribution parameters

$$D = \begin{cases} 0 & \text{no fish present} \\ 1 & \text{fish present} \end{cases}$$

The abundance parameter, $A_{x,y}$, was estimated by oceanic gamefish raised only, hooked, lost, or boated by the fishermen and therefore has a larger degree of bias due to the ability of anglers to identify, attract, and hook the fish. The distribution parameter, $D_{x,y}$, by its definition was less susceptible to error than the abundance parameter, $A_{x,y}$, and therefore was utilized in the mathematical modeling efforts.

Data Preparation. Resource information was available for only 34 out of the 54 fishing squares on August 4 and 30 out of the 54 squares on August 5. However environmental information was not obtained from some squares for which there was catch data. Accordingly, an averaging technique was used to provide environmental information for those squares where resource data had been recorded. The technique consists of averaging the values of all encircling squares and has previously been used for interpolating catch data (Wise and Davis, 1973). Furthermore, individual test square values for each parameter were computed by averaging all station readings in that square for that parameter each day. Environmental data for each square fished consisted

of the following parameters: surface water temperature, surface salinity, air temperature, Secchi extinction depth, sea state, Forel-Ule water color, chlorophyll-a, chlorophyll-b, chlorophyll-c, water depth, and distance from shore. These parameters were utilized as independent variables in the initial correlation analyses. Atmospheric pressure was eliminated from the analyses because of the limited number of stations for which this measurement was reported.

The billfish (blue marlin, white marlin, sailfish) were selected as the resource to analyze because of the lack of catch data on the tunas and the lower priority level given to the dolphin and the wahoo. Further analysis revealed that insufficient catch data for the blue marlin did not warrant continuing effort on that species. Efforts were therefore concentrated on white marlin and sailfish and only the white marlin results are presented in this paper.

Initial correlation analyses were made to determine which form of the resource abundance and distribution parameters (fish raised only, hooked raised plus hooked, or boated) should be used. The hooked parameter was found to have the strongest correlation with the environmental parameters. This stronger correlation can be explained by the lesser degree of bias of this measurement as compared to the raised parameter, i.e., there is less chance of incorrect identification once the fish is hooked. Conversely, the boated parameter, which had no possibility of identification error, caused a significant bias in the distribution parameter, $D_{x,y}$, when the fish was hooked but not boated. Therefore, the hooked form of the parameter was used in correlation analyses and mathematical modeling.

Further bias was identified in the resource distribution parameter in that a certain level of fishing pressure was required to determine if there were fish in a fishing square. In other words, if fishing pressure was insufficient in a square with environmental characteristics conducive to fish and in one with environmental characteristics not conducive to fish, both would have a value of 0 for the distribution parameter regardless of the presence of fish. This would tend to conceal relationship between the resource and environment. Having found that no white marlin or sailfish were caught in any of the test squares with less than 4 boat hours of fishing pressure, a correction for this bias was made by eliminating from the analyses all squares having less than 4 boat hours of fishing pressure. This resulted in narrowing the study to 24 out of the 34 test squares remaining for August 4, and 22 out of the 30 remaining for August 5.

Correlation Analysis. Correlation and regression techniques were utilized to define relationships between the resource and the environment as defined by sea truth measurements. The number of white marlin hooked in each test square was utilized as a measure of abundance ($A_{x,y}$) and converted to form the distribution parameter ($D_{x,y}$). Linear correlation coefficients were computed for white marlin abundance and distribution and each of the environmental parameters (Table IV) measured on both August 4 and August 5, 1973. The results listed in Table IV show a difference between abundance and distribution and probably reflect bias in the abundance parameter. The dubious quality of the abundance parameter led to emphasis on the distribution parameter in the modeling efforts. It should be stressed here that the correlation coefficients are a measure of the linear relationships between the given dependent variables and each environmental parameter respectively, and do not necessarily indicate the set of parameters which should be used in developing predictive models. This is due to the fact that in some cases the parameters listed are also statistically correlated. For example, in the test area, water depth and distance from shore have a correlation coefficient of .8328 which is significant at the 99% level. Hence, these two parameters are not statistically independent and one or possibly both (depending on interrelation with other parameters) may not be selected as a model parameter. However, the correlation coefficients listed in Table IV provide a measure of the linear relationship (within this set of data) between the white marlin parameters and each of the environmental parameters.

Assignment of biological significance to these correlations was not within the scope of this study. The parameters measured may only be serving as indices of unmeasured parameters. Other investigators (Gibbs, 1957) have also found temperature to be related to fish distribution. In analyses of the distribution of white marlin, Gibbs found that successful white marlin longline sets were made in surface water temperatures above 24°C.

TABLE IV. CORRELATIONS between white marlin (hooked) abundance ($A_{x,y}$) and distribution ($D_{x,y}$) estimates and sampled environmental parameters (E).

Parameter	Degrees of Freedom	Correlation Coefficient (r)	
		Distribution	Abundance
Water Temperature (°C)	44	.407***	.310**
Salinity (ppt)	44	-.145	.001
Air Temperature (°C)	44	.113	.218*
Secchi Transparency (m)	44	.129	.269**
Sea State (m)	44	.272**	.183
Forel-Ule Color (units)	44	-.180	-.044
Chlorophyll-a (mg/m^3)	44	.200*	.054
Chlorophyll-b (mg/m^3)	44	.056	-.005
Chlorophyll-c (mg/m^3)	44	.214*	.241*
Water Depth (m)	44	.329**	.170
Distance from Shore (km)	44	.454***	.323**

* 90% significance level
** 95% significance level
*** 99% significance level

Since the fishing data were collected in August when the Gulf is nearly uniform in temperature, 29°C (Gulf of Mexico Fishery Bulletin 89), the large catch of white marlin was not unexpected A factor which should be noted here is that there was a correlation coefficient of .407 significant at the 99% level for white marlin distribution and temperature with all of the sampled temperatures measuring between 28.5°C and 31.6°C. The strong positive correlation held true for data taken on both days as well as the combined data sets.

There was no evidence of correlation of either distribution or abundance with depth of water according to Gibbs. Thus, the apparent strong depth correlation listed in Table IV may be valid only in this particular test area and may be seasonal or coincidental.

Positive correlations (significant at the 90% level) between white marlin distribution and the chlorophyll-a and -c (phytoplankton measurements) were found. This may be compared with a study of white marlin in the Middle Atlantic Bight where important marlin areas showed distinctly high zooplankton volumes (Sylva and Davis, 1963). The comparison supports both positions if it is assumed that small fish feed on both types of plankton and, in turn, white marlin prey on these small fish or fish attracted by these fish.

Remotely Sensed Oceanographic Parameters and Correlations with the Environment

The object of this phase of the experiment was to measure from aircraft and satellite water surface temperature, turbidity, and chlorophyll concentration. Techniques currently under development in the NASA Earth Resources Laboratory are being used for the measurements.

Sea Surface Temperature. The remote measurement of sea surface temperature has been widely studied. Absolute accuracies of 0.5°C are readily obtainable from aircraft measurements using one, or in some cases no ground truth calibration. (Boudreau, 1972a; Boudreau, 1972b; Daughtery, 1973; Worthington. 1973). The same techniques used in the aircraft measurements were to be applied to Skylab thermal data acquired over the test area.

The aircraft thermal data were taken from 3000 meters with an RS-18 scanning radiometer and a PRT-5 radiometer and also from 6100 meters with another PRT-5 radiometer. These radiometers are sensitive in the 8-14 μm regions of the spectrum. The aircraft thermal data have been processed and a radiometric temperature trace along the flight lines developed. From this trace, the temperature at points between the flight lines has been interpolated to provide the basis of the contour map shown in Figure 4. For comparison purposes, the contour map of surface temperature determined by surface measurements and corrected for insolation during the ten-hour period of sampling to a time midway through the remote data acquisition exercise is presented as Figure 3. The time correction was performed by computing the change in temperature averaged over the test area on an hourly basis and adding the appropriate change to readings made at times different from the normalization time. A composite of the thermal data from the two aircraft was made to fill in gaps that occurred in different locations along the flight lines for the two aircraft caused by time-varying cloud cover. There were, however, several locations along the flight lines where clouds caused a total loss of data, and other locations where anomalous temperature measurements may have resulted from the fact that the atmosphere was not homogeneous to the extent that is required by the algorithm for correction of atmospheric effects.

Comparison of the surface and remote temperature contour maps shows that, while they are not identical, the same basic trends are present in both maps. There are two likely explanations for the discrepancies. The surface measurements were made by many individuals under different conditions, which could easily result in measurement errors of up to $0.2^{\circ}C$ (Worthington 1974). Because of the $0.25^{\circ}C$ contour interval, errors of this magnitude would distort the contour patterns. A second explanation is the heterogeneous atmosphere perturbing the remotely measured surface temperature. This is a consequence of uncertainty of knowledge about the atmosphere over the extensive test area.

It was anticipated that Skylab S192 data would provide thermal measurements over the entire test area. However, the test site was 40-70% clouded at the time of the Skylab overpass and no S192 data in computer compatible form has been received. Thus, there has as yet been no effort to utilize the wide area coverage of the Skylab thermal sensor.

Chlorophyll. Measurement of chlorophyll-a concentration obtained from radiance measurements has been attempted with varying degrees of success by many workers (Clark, 1970; Hovis, 1973; Weldon, 1973). No technique has apparently achieved either sufficient accuracy or consistency to be generally accepted as the best remote measurement method. The remote data processed in the study thus far was obtained by an Exotech 20-D spectral radiometer, flown on the light aircraft at 3000 meters. The instrument, as configured for this experiment, measured radiance in the region of the spectrum from 390 to 1100 nanometers (nm) and calibrated at 57 wavelengths in that range.

An algorithm for computing chlorophyll-a concentration developed by Weldon (1973) has been used successfully with data taken with this radiometer, but at lower altitudes over the Mississippi Sound. Weldon's technique consists of a linear function of the difference between the radiance at 620 and 470 nm, normalized by the radiance at 520 nm. The coefficients of the function are determined from ground truth data.

$$C_W = \alpha_1 (R_{620} - R_{470})/R_{520} + \alpha_2 \qquad (1)$$

This algorithm was applied to the data acquired in this experiment. The root mean square (rms) deviation of these calculations from the surface measurements was $0.48\ mg/m^3$ for 18 measurement points, of which nine were used for calibration.

Principal factor analysis of the entire 57 wavelength spectrum normalized by the 520 nm radiance indicated that the entire spectrum could be reconstructed from only six measured wavelengths with the radiance at each wavelength for all the spectra reproduced with an average deviation of 0.5%. From the surface chlorophyll-a measurements, a set of six coefficients for Eq. (2) were determined which gave a second remote chlorophyll-a measurement.

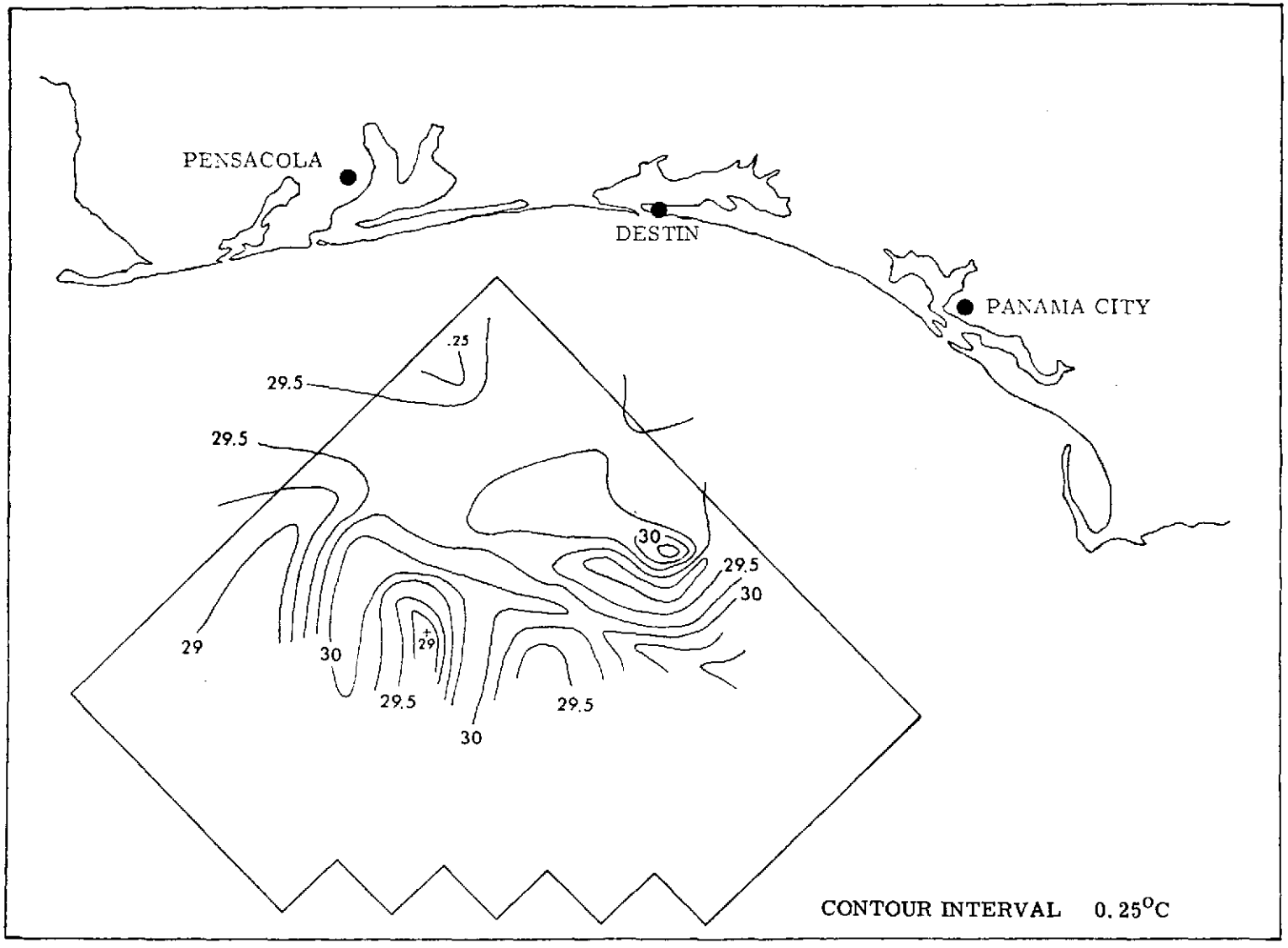

FIGURE 3. SURFACE MEASUREMENT OF WATER TEMPERATURE

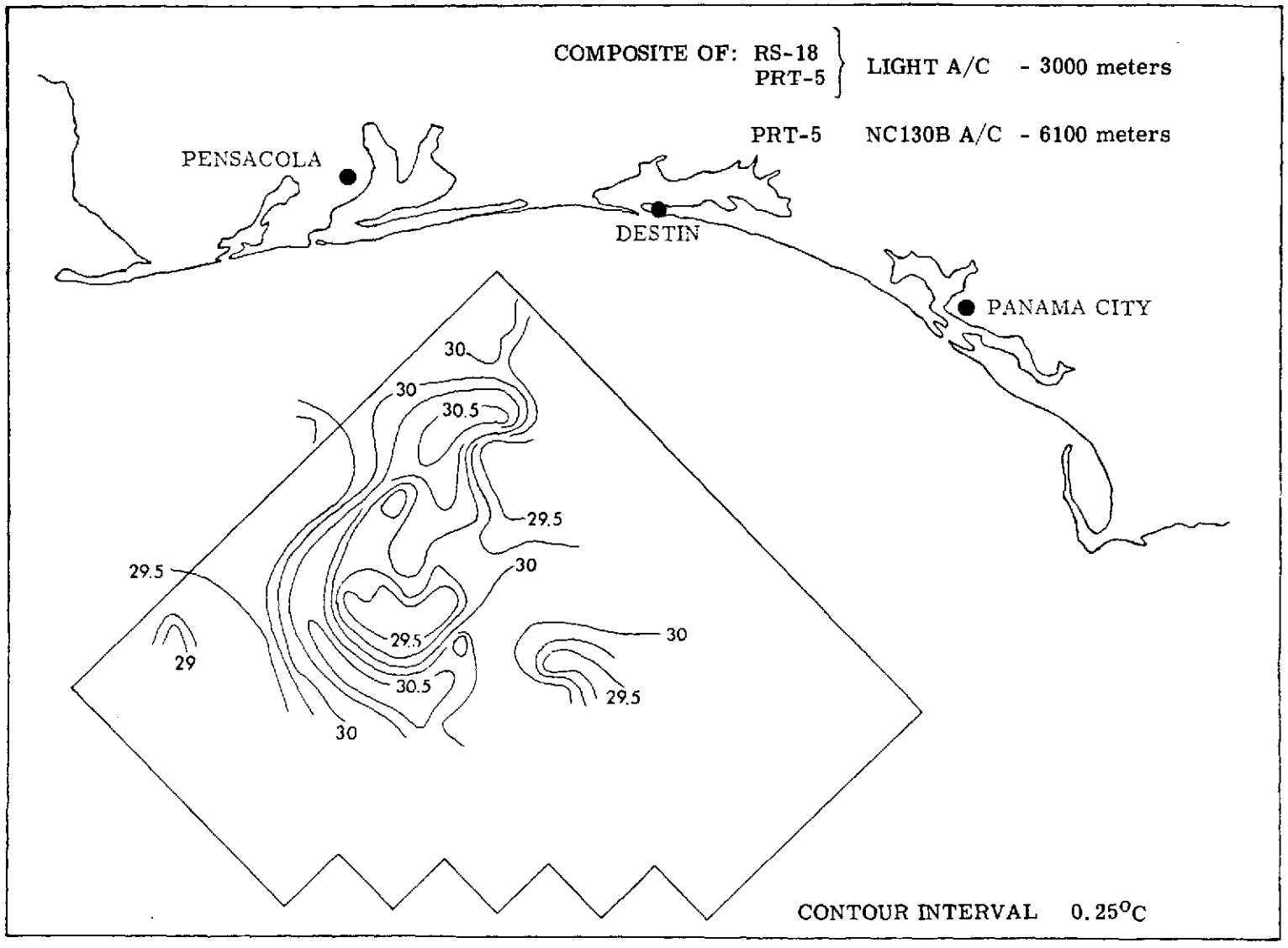

FIGURE 4. REMOTE MEASUREMENT OF WATER TEMPERATURE

$$C_P = \sum_{n=1}^{6} \alpha_n R_{\lambda_n}/R_{520} \quad (2)$$

where λ_n = 480, 560, 630, 769, 911, and 1073 nm

There were frequently substantial differences between the values obtained by application of this algorithm and those obtained by the first technique. The rms deviation for this calculation was 0.69 mg/m^3 for 18 measurements, of which nine were used for calibration.

Principal factor analysis determines the factors which best account for the total variability of the spectral data. The information content was maximized by this technique rather than optimized. A third technique was used to optimize the information content and minimize the number of wavelengths. Examination of the correlation of the 520 nm normalized radiance at each of the 57 wavelengths indicated that the chlorophyll-a concentration was not highly correlated with the radiance at 470 and 600 nm. Further analysis showed that a linear combination of these radiance values correlated very well with the square of the chlorophyll-a concentration, so a third calculation of the chlorophyll-a concentration based on spectral radiometer measurements was made using the relation shown in Eq. (3).

$$C_c = \sqrt{\alpha_1(R_{600} - R_{470})R_{520} + \alpha_2} \quad (3)$$

Figures 5 and 6 are the contour maps drawn from the surface and remote measurements of chlorophyll-a, respectively. The remote measurements are a composite of the results of the first and third calculation. Careful examination of the two sets of measurements showed that the third gave better results in areas where chlorophyll-a content was low (0.28 mg/m^3 rms error), but that the response flattened out at concentrations above 2.3 mg/m^3. The first technique was better at the higher concentrations, so when a concentration greater than 2.0 mg/m^3 was indicated by the third technique, the value predicted by the first technique was used; otherwise, the value was that computed from Eq. (3). The rms deviation of the composite at the 18 surface comparison points was 0.44 mg/m^3.

Comparison of Figures 5 and 6 shows that, while the maps do show significant differences, the large variations present in the surface data are also found in the remote data. In addition, there are some rapid changes indicated in the remote data which are not seen in the surface data. This does not require that either measurement be in error, as the remote data is a continuous sampling while the surface measurements are separated by roughly an hour's cruise. Another factor to be considered is the 10% repeatability factor (Jones, 1973) of the surface chlorophyll-a determination. It must also be remembered that no corrections for atmospheric conditions were made. These conditions were not constant over the test area, and clouds and cloud shadows do affect the apparent color and hence the inferred chlorophyll-a content.

Turbidity. For this experiment, measured turbidity was expressed as Secchi extinction depth. This surface truth measure of turbidity was used because of operational considerations, i.e., the technique is simple and the necessary equipment inexpensive. However, the measurement is subjective because of the human factor involved and is thus susceptible to considerable error.

Weldon (1973) developed an algorithm for computing Secchi extinction depth from spectral radiometer measurements, so the first attempted remote measurement of turbidity was with this technique. Weldon found that the Secchi extinction depth was proportional to the ratio of the radiance measured at 600 nm to that at 550 nm, but application of this algorithm to the data acquired in the Gamefish experiment was notably unsuccessful. The failure of this previously verified technique is probably due to the fact that Weldon's work was done with measurements made in the Mississippi Sound where three meters is generally the greatest Secchi depth observed, as opposed to thirty in the Gulf.

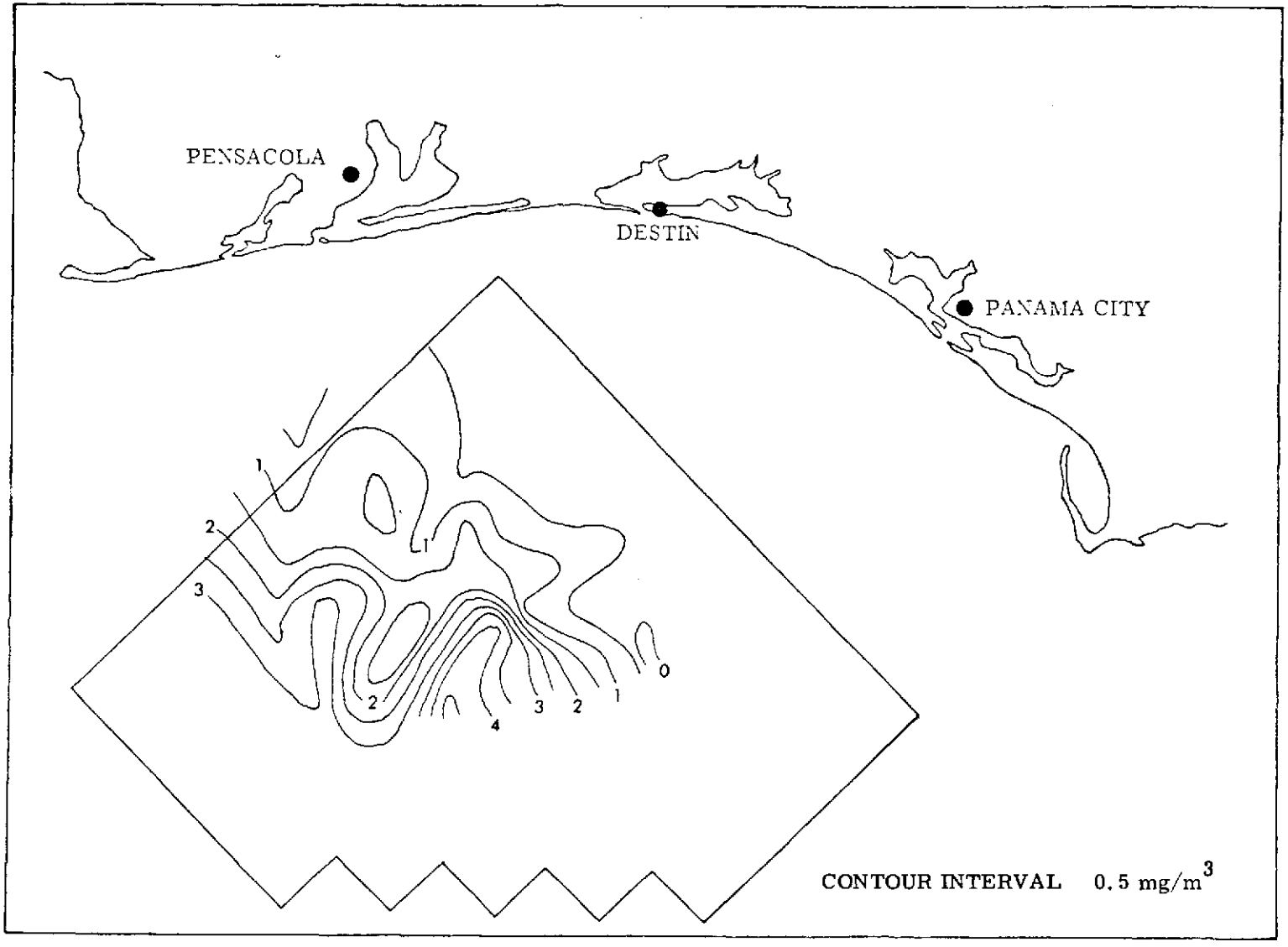

FIGURE 5. SURFACE MEASUREMENT OF CHLOROPHYLL-a

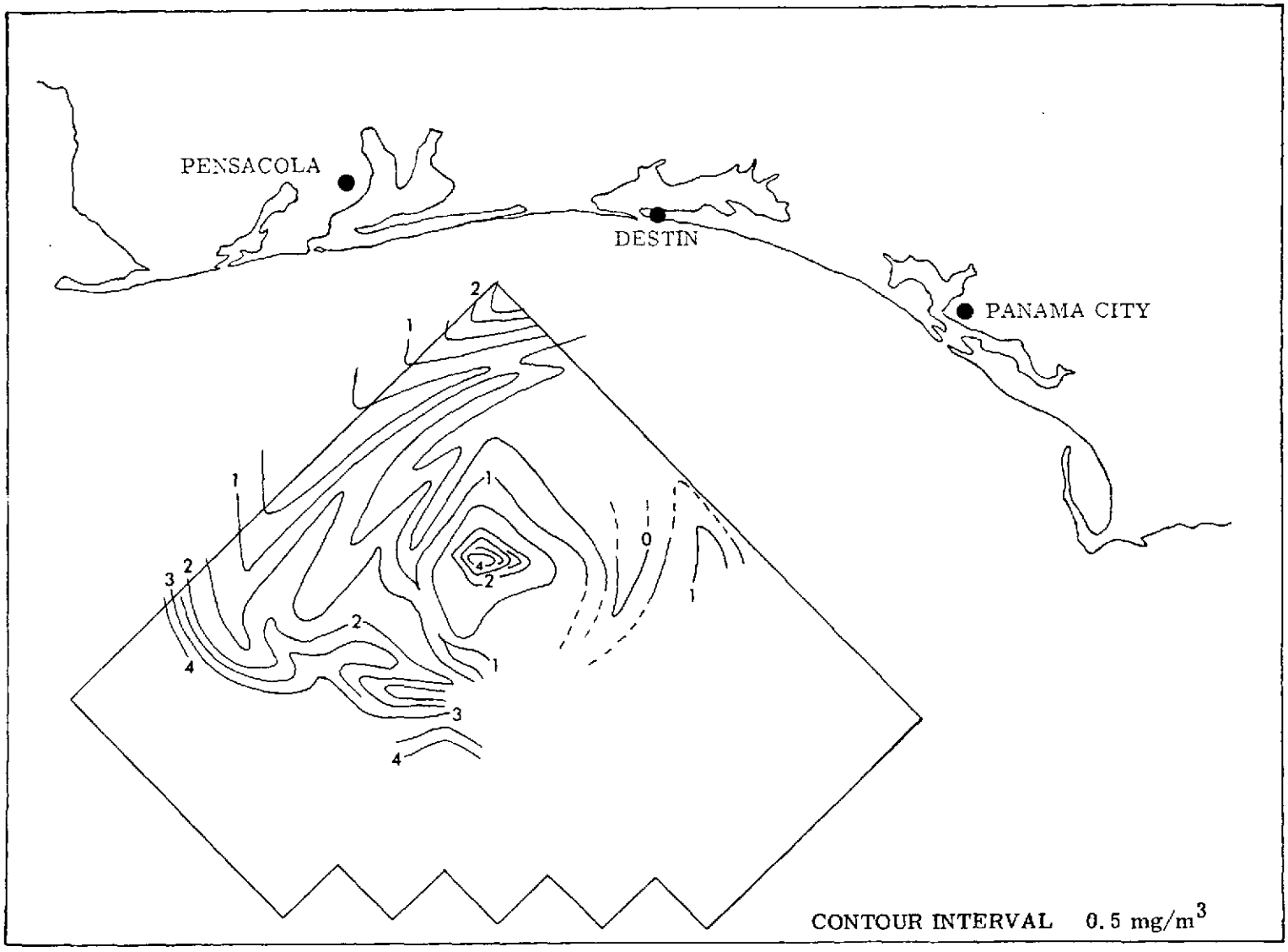

FIGURE 6. REMOTE MEASUREMENT OF CHLOROPHYLL-a

Three subsequent techniques were developed to infer turbidity measurements from the spectrometer data. The first is a simple ratio technique identical in form to Weldon's but utilizing different portions of the spectrum (420 and 570 nm). The relationship used is

$$S_w = \alpha_1 R_{420}/R_{570} + \alpha_2 \quad (4)$$

The second method again makes use of principal factor analysis performed on normalized radiance data. For the turbidity measurement, the radiance data was normalized by the radiance averaged over the entire spectrum from 390 to 911 nm, the portion of the data on which the analysis was performed. Six wavelengths were selected that would reconstruct the spectrum on a wavelength by wavelength basis for all sample spectra, to 99.95% average accuracy. A linear combination of the radiance at these wavelengths was then fit by the least squares technique to the surface measurements. The wavelengths used were 440, 490, 560, 630, 748, and 867 nm.

The third algorithm as in the chlorophyll calculation optimized the information content relative to the Secchi transparency measurement. This optimization was performed by selecting wavelengths which showed the highest correlation with the Secchi depth and the least correlation with each other. Unnormalized radiance data, radiance normalized by a wide band in the blue (390-430 nm) region, and radiance normalized by a wide band in the infrared (911-1073 nm) region was examined. The best set of correlations was found with three wavelengths (410, 440, and 550 nm) of the blue-normalized radiance. An expression of the form

$$S_c = \sum_{n=1}^{3} \alpha_n R_{\lambda_n}/R_{blue} + \alpha_4 \quad (5)$$

was used to calculate the Secchi extinction depth.

Despite the fact that the coefficients of the three relations differ drastically, the three sets of calculations agree closely, generally with less than 10% deviation. The results are in agreement with the surface measurements as can be seen from Figures 7 and 8 which are contour maps of the Secchi extinction depth made from surface and remote measurements according to the third technique. While the calculated rms error was 3.9 meters for 20 points, of which eight were used for calibration, the trends were well represented. The chief discrepancy between the two is in the area where surface readings on the order of 30 meters were made and where the remote measurement indicates greater turbidity.

There are two likely explanations for this variation. Because of the criteria used in selecting calibration points for the remote measurements, which included a maximum time difference between surface and remote measurements of three hours, no calibration points had Secchi depths of more than 17 meters. This would introduce an uncertainty of unknown magnitude into measurements outside the calibrated range. Also, reports from the surface observers indicated that water conditions were changing over the test area. It is thus possible that the sea conditions changed at this sample station during the four hour interval separating surface and remote measurements.

Salinity. Because salinity is an important factor in the white marlin predictor to be described later, it would have been desirable to use remote measurements of salinity in this experiment. The feasibility of applying L-band radiometer data to measure salinity remotely has been demonstrated by Thomann (1973). Unfortunately, the microwave radiometer necessary for this measurement was not available for use on the aircraft for this experiment; the other potential source for remote salinity measurements was the L-band radiometer on Skylab.

Generally the state of the art satellite measurement of surface salinity in the microwave spectrum is not feasible. In open ocean areas the 1-2 ‰ sensitivity of the remote measurement is insufficient to measure the small salinity gradients generally encountered. In coastal waters where strong salinity gradients are present, it is difficult from satellite altitudes to get data which is sufficiently free of land contamination. While surface measurements indicated that there were salinity gradients within the test area that would be within the sensitivity limits of the microwave technique, the land contamination will undoubtedly negate the effectiveness of the system. In addition the footprint of the instrument is almost as large in area as the entire test site, resulting in insuffient resolution. When the S194 data are received, the data will be analyzed but it is doubtful that meaningful data will be obtained.

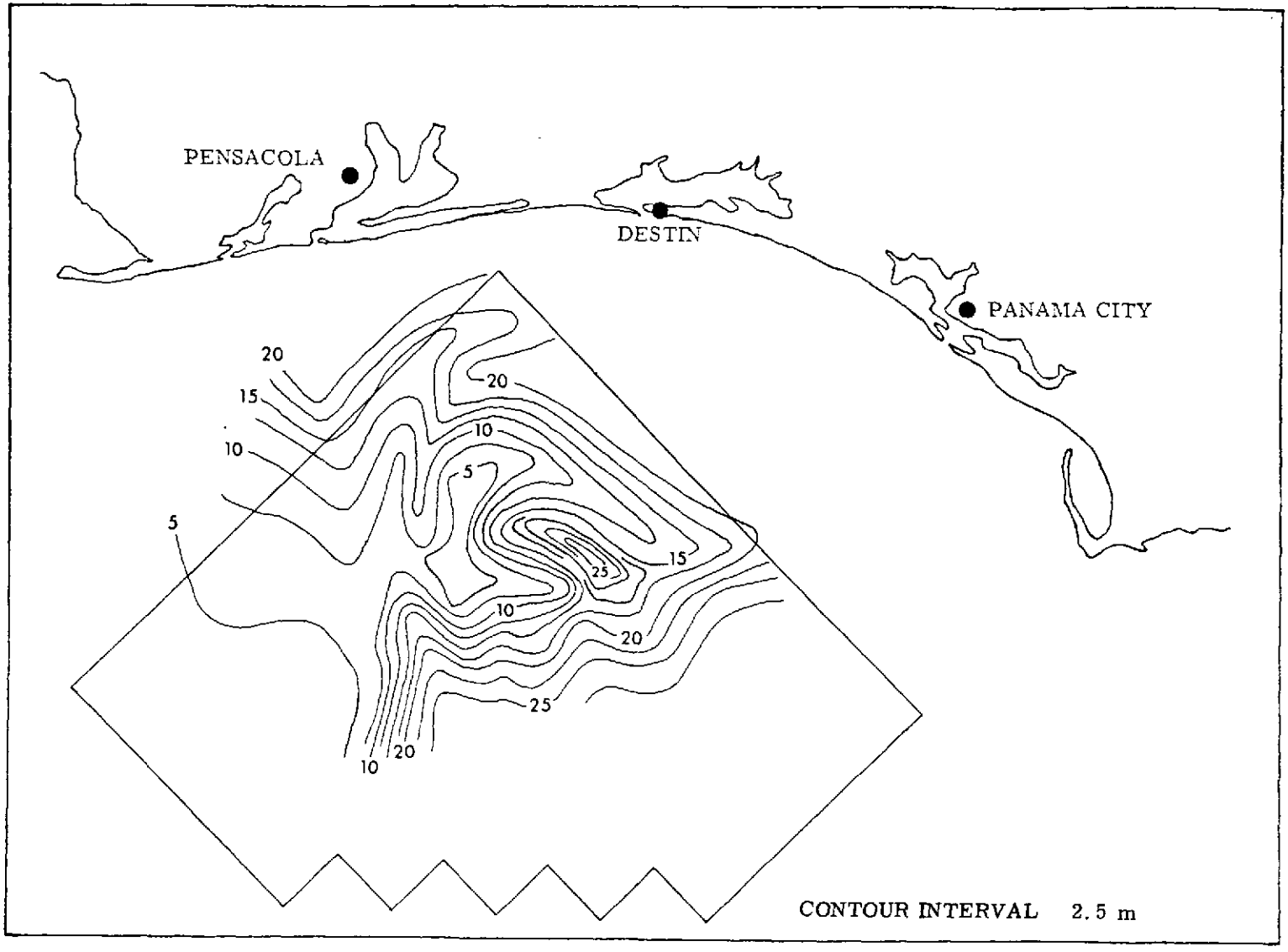

FIGURE 7. SURFACE MEASUREMENT OF TURBIDITY (SECCHI EXTINCTION)

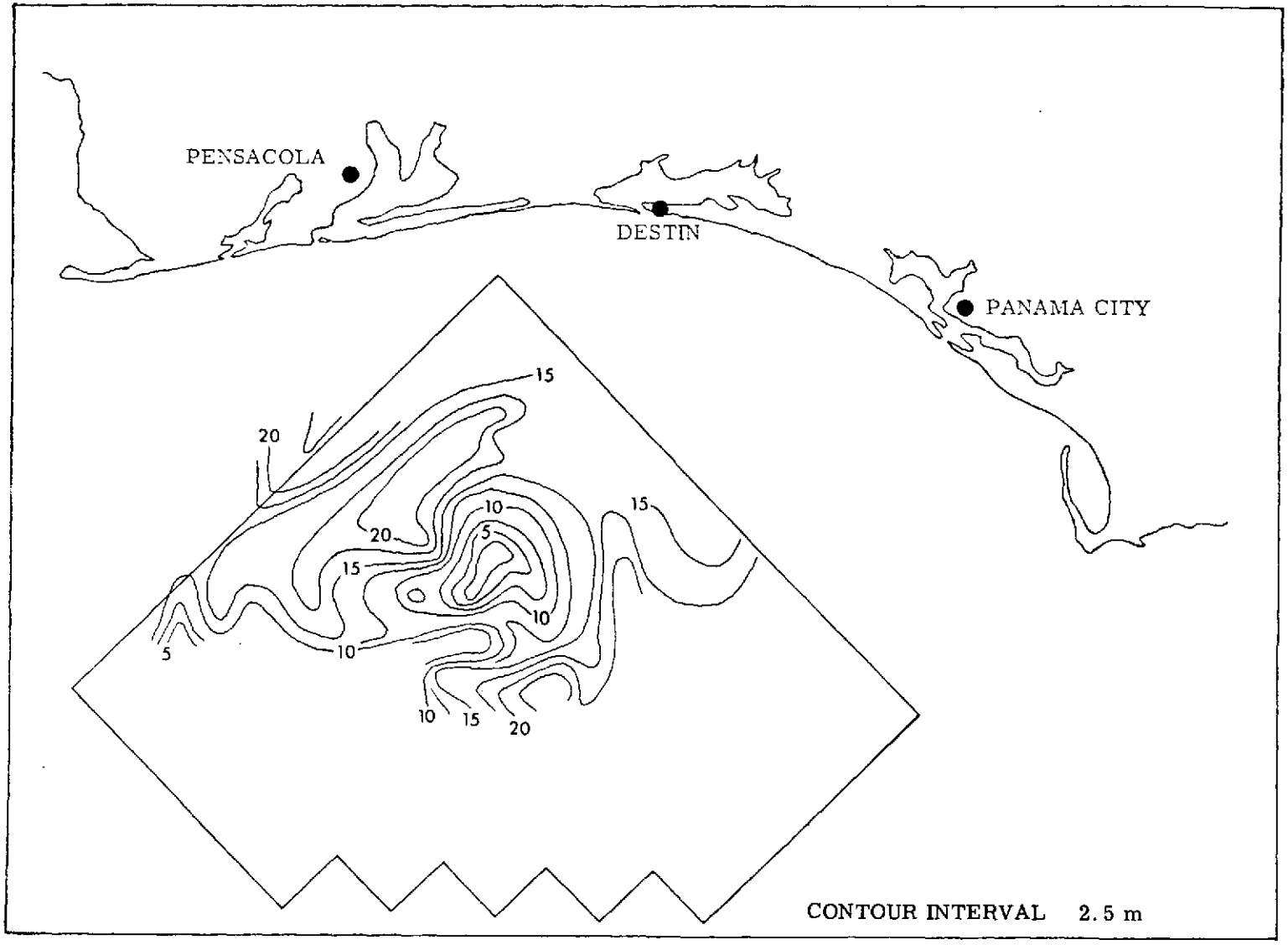

FIGURE 8. REMOTE MEASUREMENT OF TURBIDITY

Resource and Remote Data Relationships

Approach. Fishermen in search of gamefish consider, as a rule, the color of the sea as the primary indicator of good fishing grounds. The generally accepted theory is that the gamefish are found principally in areas where the water is blue as opposed to green. The approach taken in attempting to define a relationship between the billfish resource and marine phenomena directly sensible by the satellite and aircraft sensors utilized visual interpretation, color enhancement of multiband photography, and direct correlation between spectral radiometer "color" measurements and resource distribution information.

Water Discontinuities. The photography from the NC-130B and the light aircraft were visually examined for surface discontinuities which would indicate the boundary between different water masses. The discontinuities searched for were either sharp changes in water color, of which none were found, or surface rips. Many rips were identified, some in both sets of aerial photography. Unfortunately, the portion of the test site visible in the photography was small, so much of the study area could not be included in this analysis of the aerial photography.

Figure 9 shows the fishing squares in which rips were found in the photography. The fishing squares containing rips are indicated by horizontal lines. Squares where fish were hooked are shaded. The limited data set does not permit any definitive conclusions to be drawn concerning fish/rip relationships.

No rips were found in the Skylab S190A photography which has been examined in detail. This is to be expected since these surface features generally have widths less than the resolution of both the S190A and S190B products.

Water Color. Areas of blue and green water should have been distinguished using the aerial photography, but problems such as clouds and improper filters rendered this photography useless for color determination. The E20-D spectrometer data show several areas where the indicated water color shifted between blue and green. While it is difficult to conceive the actual "color" viewed by the instrument from the resulting spectrum, it is possible to infer changes in color from changes in a series of spectra. For example, in the case of typical sea spectra, as the radiance in the 550 to 600 nm region decreases while the radiance in the 400 to 500 nm region increases, the color shifts towards the blue. Several spectra which illustrate this color variation are shown in Figure 10.

The object of this phase of the analysis is to directly relate the water color as defined by the spectral radiometer to the fish distribution, whereas previously described analyses have concentrated on relating water color to chlorophyll and turbidity, and relating sea truth to resource distribution. This direct correlation has not yet been performed but is currently in its initial stages.

Color Enhancement of Multiband Photography. The successful correlation of menhaden distribution with particular radiation intensity levels of ERTS-1 multispectral imagery (Kemmerer et al, 1973) suggested that density slicing of S190A black and white multiband photography might be productive in this experiment. Since data in three channels of the S192 multispectral scanner were available in the form of film images, the same analysis procedure was considered, but uncorrected scene distortion was of sufficient magnitude to render these products unsuitable. Another potential source of information was the S190B (Earth Terrain Camera) sensor data. However, the only photographic data available from this sensor system were high resolution aerial color (0.4-0.7 μm) paper prints which did not reveal any sea surface pattern differentiation.

Method of Analysis. Of the S190A film products acquired and received for analysis, black and white (B&W) 70 mm negative transparencies of successive frames 242 (11:41:04.3 local time) and 243 of the S190A sensor system in spectral bands 0.5-0.6 μm and 0.6-0.7 μm were ultimately chosen for detailed analysis. Selection of these frames were made on the basis of image quality, test site accommodation and potential for revealing sea surface differentiation. Neither frame selected would accommodate the entire test site area.

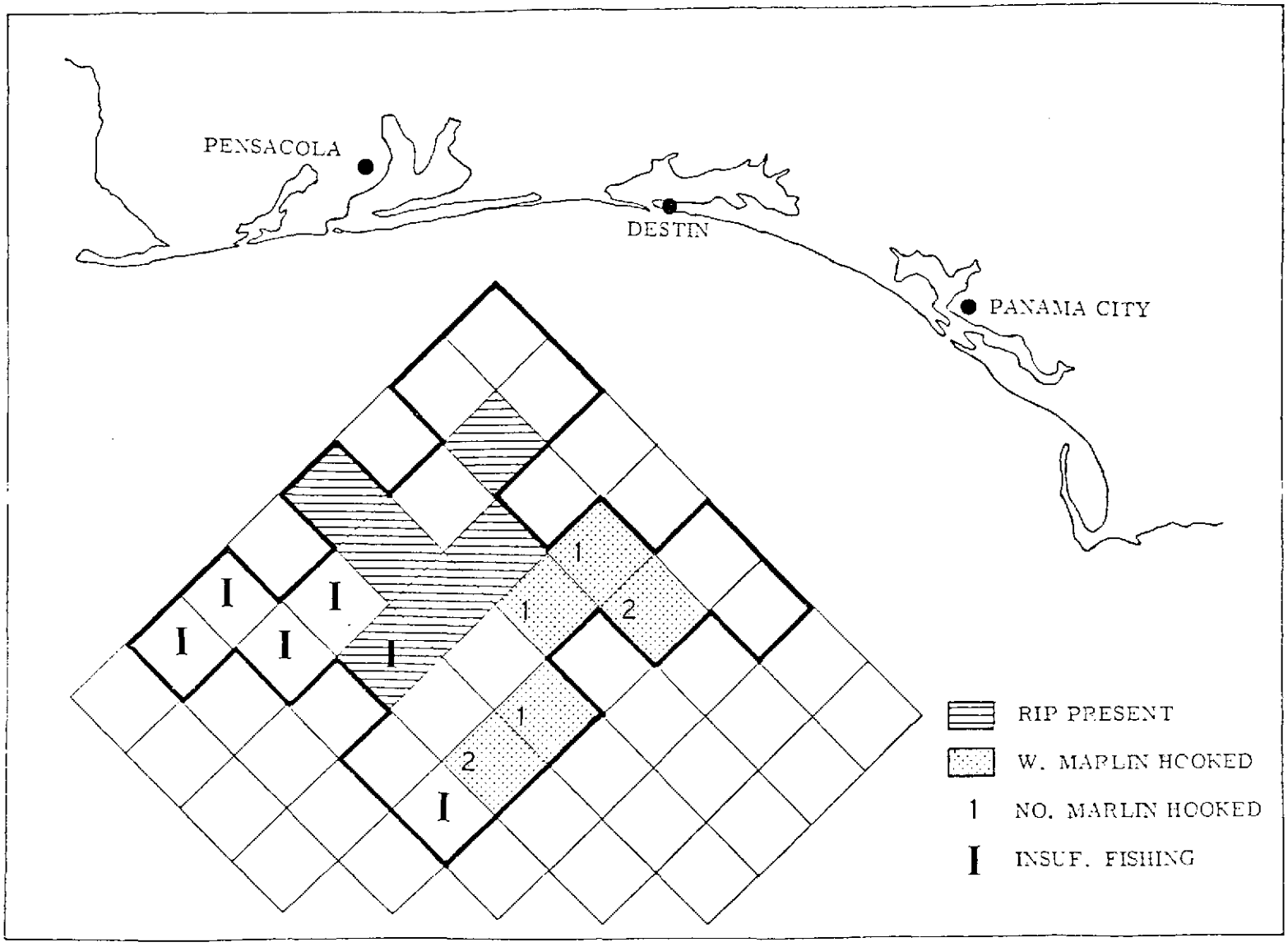

FIGURE 9. COMPARISON OF WHITE MARLIN DISTRIBUTION WITH SURFACE RIP LOCATIONS

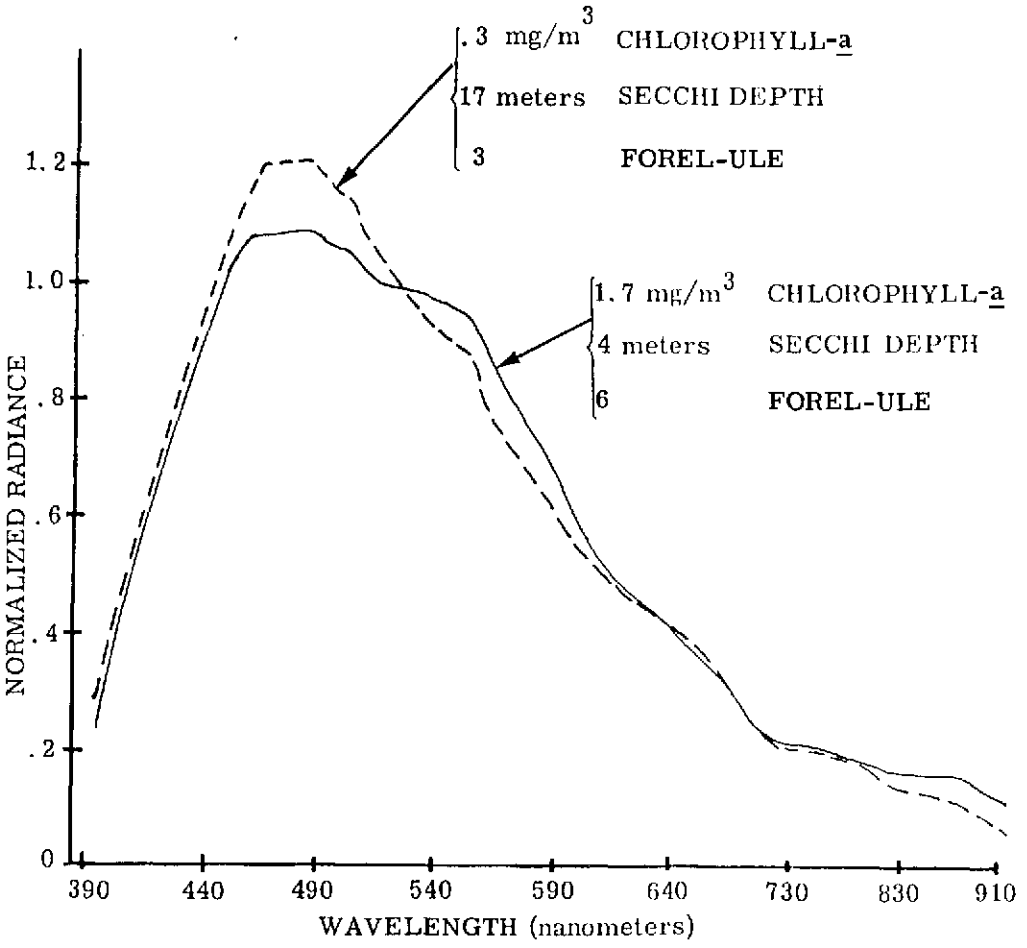

FIGURE 10. COMPARISON OF SPECTRA OF BLUE AND GREEN WATER

Analysis Results. The only Skylab sensor products available, as well as suitable, for analysis were photographs from the S190A sensor system. As previously noted, only two of the six S190A spectral band photographic products were utilized for detailed analysis. The remaining four, i.e., 0.7-0.8 μm (IR B&W), 0.8-0.9 μm (IR B&W), 0.4-0.7 μm (HR Aerial Color), and 0.5-0.88 μm (IR Color) did not reveal any sea surface differentiations.

Both the 0.5-0.6 μm and the 0.6-0.7μm band products were density sliced to derive sea surface information. In comparing the distribution of hooked white marlin per square for 5 August a false color image containing five density slices (not shown because of color reproduction costs and image information degradation in the color to black and white conversion) it was apparent that some fish were hooked in squares (25, 28, 31 and 45) revealing two different classes of surface water color. The fishery resource data, as summed and positioned to the center of the squares, therefore could not be correlated with any particular density slice of the S190A multiband Skylab photography as originally anticipated. This assertion, however, has not precluded ongoing analysis to relate usable Skylab data to the acquired sea truth environmental information.

The S190A photographs also revealed a number of anomalous dark patches (McClain and Strong, 1969) within the sunglint areas, the largest of which appears in grid square numbers 31 and 48. This particular patch is oval shaped; encompasses a total area of about 570 square kilometers and is associated with calm sea state measurements ranging from 30 to 40 cm.

PREDICTION MODELS

Model Development

Multiple regression analysis was used to develop models to predict white marlin distribution ($\bar{D}$) in the Skylab test area. Initial runs utilized the eleven parameters listed in Table IV along with all possible interactions (formed by computing the products of each parameter pair) as the indepedent parameters. The first models D_1, D_2, D_3 listed in Table V were constructed utilizing data collected on August 4, on August 5, and the combination of August 4 and August 5. These models were developed based on five parameters: surface water temperature (T), Secchi extinction depth (C), salinity (S) and the two interaction parameters, the product of Secchi extinction depth and chlorophyll-a, (CA), and the product of salinity and surface water temperature (ST). Comparison of constant terms and coefficients (by magnitude and sign) in models D_1, D_2, and D_3 reveal extreme difference or instability from day to day. Therefore, it appeared that important information was not considered, a combination of linear terms was not sufficient to model the day to day changes, or a white marlin distribution model could not be developed.

Additional work was initiated to try to stabilize the models. Water density was computed and substituted for the product of water temperature and salinity. The latter two had been used in the earlier regression runs. A measure of water density (σ_t) was computed utilizing the following equations (Knudsen, 1962).

$$Cl = \frac{S-0.030}{1.805} \tag{6}$$

$$\sigma_o = -0.069 + 1.4708\ Cl - (1.57 \times 10^{-3})\ Cl^2 + (3.98 \times 10^{-5})\ Cl^3 \tag{7}$$

$$\Sigma_t = -\frac{(t-3.98)^2}{503.57} \cdot \frac{t+283}{t+67.26} \tag{8}$$

$$A_t = t\left[4.7867 - 0.098185t + (1.0843 \times 10^{-3})t^2\right] \times 10^{-3} \tag{9}$$

$$B_t = t\,(18.03 - 0.8164t + 0.01667t^2) \times 10^{-6} \tag{10}$$

$$\sigma_t = \Sigma_t + (\sigma_o + 0.1324)\left[1 - A_t + B_t\,(\sigma_o - 0.1324)\right] \tag{11}$$

TABLE V. EMPIRICAL REGRESSION MODELS which predict white marlin distribution (D) in the Skylab test area.

T = Water temperature (^{o}C)
C = Secchi disc transparency (m)
S = Salinity (ppt)
ST, CA = Interaction formed as the product of the respective parameters

B = σ_t (measure of water density)
where $\sigma_t \times 10^{-3} + 1$ = water density (g/cm^3)

A = Chlorophyll-a (mg/m^3)

MODEL	INCLUSIVE DATES (1973)	n	REGRESSION MODEL	STANDARD ERROR OF $\bar{D}$	MODEL CORRELATION COEFFICIENT	SIGNIFICANCE LEVEL (%)
D_1	4 August	24	$\bar{D}$ = -419.5394 + 14.3929T +12.9764S + .0567C -.4461ST + .0074CA	0.3435	0.797	99.5
D_2	5 August	22	$\bar{D}$ = 164.1002 - 5.3527T -6.3246S + 0.173C +.2071ST - .0021C	0.4996	0.499	50
D_3	4 & 5 August	46	$\bar{D}$ = -25.4052 + .9301T +.3258S + .0139C -.0133ST + .0008CA	0.4751	0.436	75
D_4	4 August	24	$\bar{D}$ = -13.3676 + .6583T +.0718C - .3651B +.0043CA	0.3589	0.762	99.5
D_5	5 August	22	$\bar{D}$ = -22.4714 + .8179T +.0143C - .1035B -.0014CA	0.4879	0.489	60
D_6	4 & 5 August	46	$\bar{D}$ = -12.8553 + .4959T +.0142C - .0950B +.0007CA	0.4693	0.436	90

where: S = salinity in ‰
t = temperature in °C
σ_t = density parameter

NOTE: Water density (g/cm^3) at observed salinity temperature and 0 meters depth (atmospheric pressure) = $\sigma_t \times 10^{-3} + 1$.

The resulting density measure σ_t was used in constructing models D_4, D_5, and D_6 which also contain surface water temperature, Secchi extinction depth, and the product of Secchi extinction depth and chlorophyll-a. Comparison of the constant term and coefficients reveals a significant improvement in the stability of coefficient of each parameter from model to model. It should also be noted that the significance level was improved on the August 5 model and the combined data model. The result indicates that the relationship between white marlin distribution and the environmental parameters is more complex than a linear combination of the environmental parameters. However, while only two days of data were available for modeling efforts, it is evident that the relationship can be modeled with reasonable stability from day to day.

Model Evaluation

The D_4 and D_5 models were tested with independent test data by using August 4 test data in D_5 (developed from August 5 data) and August 5 test data in D_4 (developed from August 4 data). In each case the resulting unnormalized predicted distribution values (Y) were separated into a low, medium and high probability ranges. This was accomplished by computing the mean ($\bar{Y}$) and standard deviation (S) of each set of predicted value. The probability ranges were fixed as follows:

Low probability = $Y < \bar{Y} - 1/2\ S$

Medium probability = $\bar{Y} - 1/2\ S \leq Y \leq \bar{Y} + 1/2\ S$

High probability = $Y > \bar{Y} + 1/2\ S$

Each predicted value for each test square was classified as low, medium or high depending on the probability range in which it fell. The actual distribution value for each test square was assigned a high probability if it had a distribution value of 1 and a low probability if it had a distribution value of 0.

A summation of the predicted and actual distribution values is presented in Tables VI and VII for August 5 and 4 respectively.

TABLE VI. EVALUATION SUMMARY for August 5 predicted values using Model D_4

A	P	N		
H	H	5	$\frac{14}{22} = 63.6\%$	correct
L	L	9		
H	M	2	$\frac{3}{22} = 13.7\%$	no decision
L	M	1		
H	L	2	$\frac{5}{22} = 22.7\%$	incorrect
L	H	3		

TABLE VII. EVALUATION SUMMARY for August 4 predicted values using Model D_5

A	P	N			
H	H	5	$\frac{14}{24}$	= 58.3%	correct
L	L	9			
H	M	5	$\frac{9}{24}$	= 37.5%	no decision
L	M	4			
H	L	0	$\frac{1}{24}$	= 4.2%	incorrect
L	H	1			

where: A = Actual
P = Predicted
N = Number of test squares
H = High probability
M = Medium probability
L = Low probability

It may be observed in Table VI that Model D_4 classified approximately 63.6% correctly, 13.7% fell in the intermediate zone (medium probability zone) and 22.7% were in error. It is evident that nine actual high probability squares of the 22 squares fished on 5 August or 45.5% were high probability ratings and the remaining 54.6% low probability. If only the eight predicted high probability test squares were fished, five of the eight or 62.5% were actually high probability areas.

Observation of Table VII indicates that Model D_5 classified approximately 58.3% correctly, 37.5% fell in the intermediate zone (medium probability zone) and 4.2% were in error. It is evident that 10 actual high probability squares out of 24 squares fished or 41.7% were high probability ratings and the remaining 58.3% low probability. If only the six predicted high probability test squares were fished, five of the six or approximately 83.3% were actually high probability areas.

Visual representations of the predicted values from models D_4 and D_5 are shown in Figures 11 and 12. The number of predicted test squares within a given range having fish are denoted by the shaded areas or solid lines. The number of predicted test squares within a given range not having fish are denoted by the dash lines. Ideally the shaded areas should cluster near the high value or high probability portion of range and the dash line areas near low value or low probability portion with a very minimum of intersection. The results shown in Figure 12 tend toward the ideal conditions, but in general, this is not shown by both sets of data due to imprecisions in both the data and the models.

The analysis of August 4 and August 5 data utilizing models D_4 and D_5 demonstrates the potential for reducing a fishing area by identifying high probability areas. For the cases in point a factor of three or four would be achieved. Furthermore, by only considering high probability areas, the overall probability of being in an area where fish may be hooked, can be increased approximately 25% in the cases discussed.

APPLICATION TO GAMEFISH RESOURCE UTILIZATION MANAGEMENT

Oceanic gamefish distribution predictive models of the type presented would clearly serve sports fishermen and resource managers. Knowledge of highest potential catch areas as a function of time will provide sports fishermen with the benefits of increased catch and decreased time and fuel expenditures. Figure 13 is an example of a prediction model product which displays fishing areas in terms of catch potential.

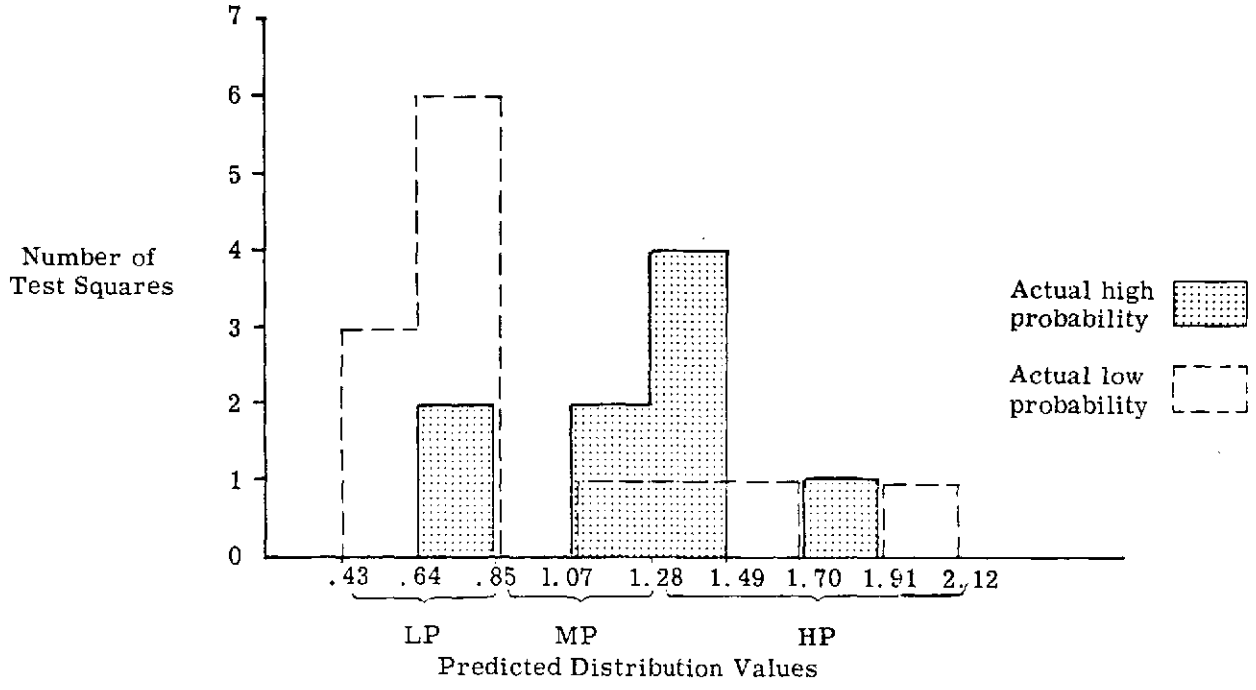

FIGURE 11. EVALUATION OF AUGUST 5 PREDICTIONS, using August 4 Model D_4

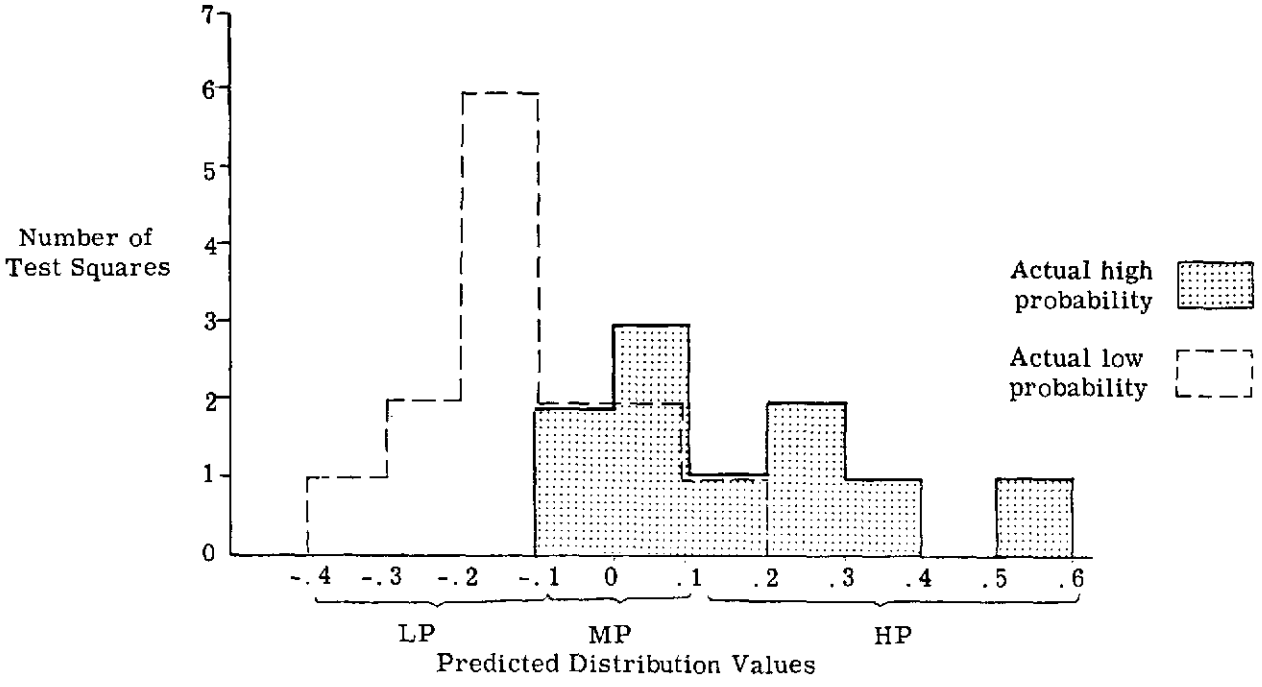

FIGURE 12. EVALUATION OF AUGUST 4 PREDICTIONS, using August 5 Model D_5

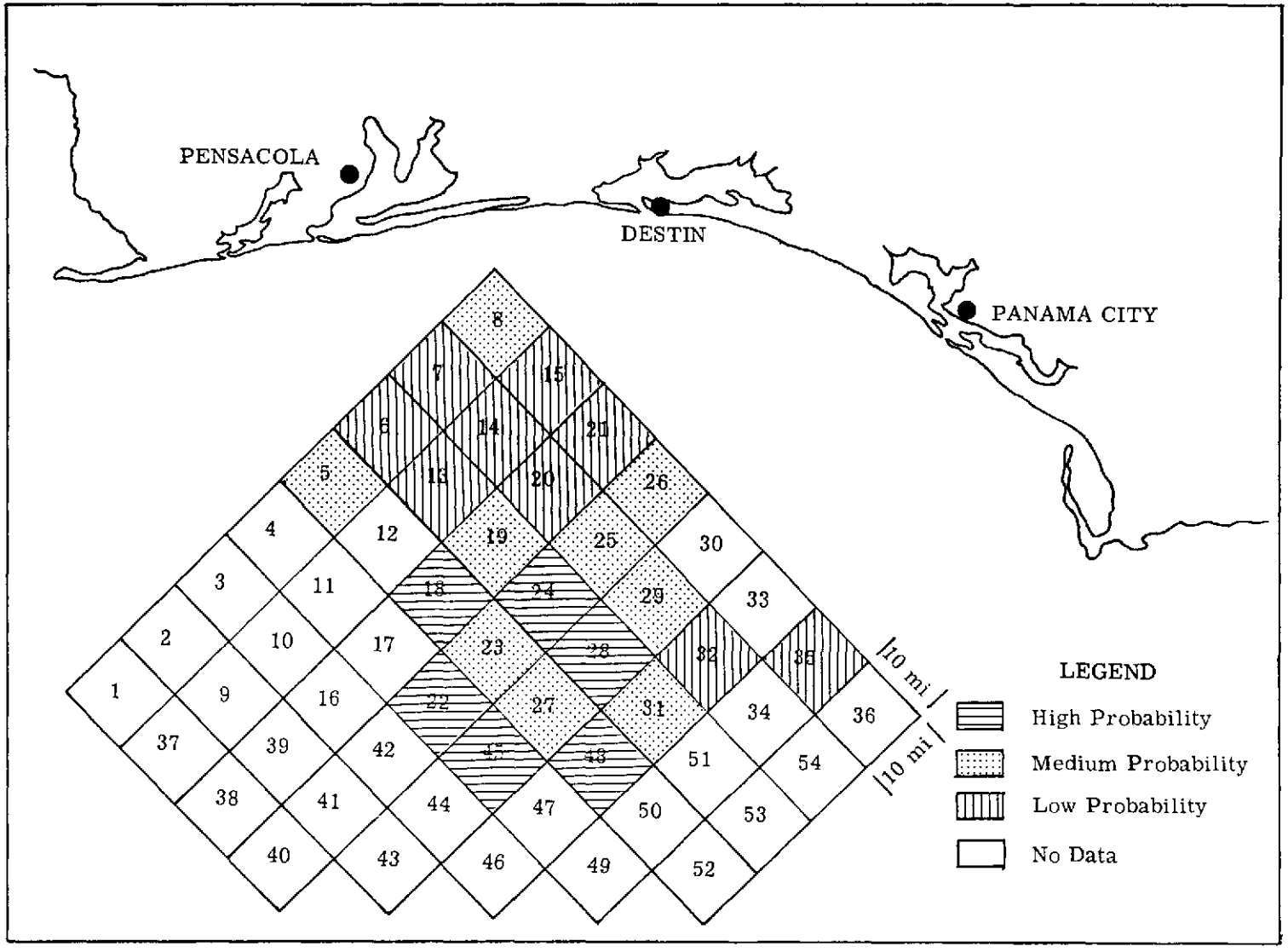

FIGURE 13. PREDICTION RESULTS OF AUGUST 4 DATA USING MODEL D_5

These predictive models are presently not adequate for resource management applications. Daily operational utilization of these models must wait until techniques for remotely sensing the necessary environmental parameters become fully functional on a synoptic basis.

As models are improved to an acceptable precision level and as repetitive data acquisition becomes economically feasible, it is reasonable to presume that these or similar models could provide the abundance and distribution information necessary for development of conservation and harvesting procedures. As operational readiness and confidence in such models are established, resource managers would have additional information on which to base domestic and international conservation decisions.

SUMMARY AND CONCLUSIONS

At this stage of analysis it appears that the distribution and abundance of white marlin show significant linear correlation with certain sea truth measurements. Immediate plans for continuing work include correlation analyses for sailfish and, perhaps, dolphin. Lack of or limited catch data precludes any effort relative to blue marlin, wahoo and the tunas.

Predictive models have been developed and have demonstrated a potential for increasing the probability of gamefishing success. They have also demonstrated a potential for reducing the search significantly by identifying areas which have a high probability of being productive. These models are currently based on catch data and sea truth information but will be evaluated with remotely sensed information in place of sea truth where possible.

Chlorophyll-a, sea surface temperature and turbidity (Secchi extinction depth) values have been inferred from aircraft sensor data. Comparisons with sea truth measurements indicate that in spite of sometimes unfavorable atmospheric conditions, reasonable accuracy has been obtained.

Cloud cover and sunglint inhibit usefulness of the Skylab imagery that has been received. An important portion of the imagery has yet to be made available for analysis. Because of these factors, which are essentially lack of data, it remains unclear if satellite sensors may be used in the models to predict gamefish abundance and distribution. However, with the successful identification of the fisheries significant oceanographic parameters and the demonstration of the capability of measuring most of these parameters remotely, the first step toward establishing the feasibility of utilizing remotely sensed data to assess and monitor the distribution of oceanic gamefish has been taken.

ACKNOWLEDGEMENT

The authors gratefully acknowledge the many participants in the investigation and those who contributed either directly or indirectly to this paper. W. H. Stevenson, as the initial Principal Investigator, gave this investigation its conceptual thrust and managed it from infancy through a complex data acquisition phase. Hundreds of charterboat captains, private boat owners, salt water anglers and marina operators enthusiastically supported field operations and voluntarily provided resource and environmental data. Dr. F. T. Neth of Pensacola Big Game Fishing Club, organized and administered an extensive gamefish tournament associated with the investigation. Individual contributors to the investigation include many from the NASA Earth Resources Laboratory, NMFS Fisheries Engineering Laboratory, The General Electric Company and Lockheed Electronics Corp., Mississippi Test Facility, Bay St. Louis, Mississippi, and the NMFS Southeast Fisheries Center, Miami, Florida. Those who contributed to the analyses and paper preparation are T. Leming, R. Holyer, G. Stephenson, H. Holly, P. Hegwood, N. Lewis and W. Bettens. The research on this paper was primarily funded through NASA Project No. 240, Contract T-8217B.

REFERENCES

Boudreau, R. D., 1972a: A Radiation Model for Calculating Atmospheric Corrections to Remotely Sensed Infrared Measurements. NASA Earth Resources Laboratory Report 14, Mississippi Test Facility, 71 pp.

Boudreau, R. D., 1972b: Correcting Airborne Scanning Infrared Radiometer Measurements for Atmospheric Effects. NASA Earth Resources Laboratory Report 29, Mississippi Test Facility, 34 pp.

Clark, G. L., Ewing, G., and Lorenzen, C., 1970: Spectra of Backscattered Light from the Sea Obtained from Aircraft as a Measure of Chlorophyll Concentration. Science, 67, pp 1119-1121

Daughtrey, K. R., 1973: Techniques and Procedures for Quantitative Surface Water Temperature Surveys using Airborne Sensors. Earth Resources Laboratory, Report 80, Mississippi Test Facility, 30 pp.

De Sylva, D. P. and Davis, W. P., 1963: White Marlin, Tetrapturus albidus, in the Middle Atlantic Bight, with Observations on the Hydrography of the Fishing Grounds, Copeia, No. 1, 18 pp.

Fox, W. W., 1971: Temporal-Spatial Relationships among Tunas and Billfishes Based on the Japanese Longline Fishery in the Atlantic Ocean 1956-1965. Sea Grant Tech. Bulletin No. 12, 77 pp.

Gibbs, R. H., Jr., 1957: Preliminary Analyses of the Distribution of White Marlin, Makaira albida (Poey), in the Gulf of Mexico. Bulletin of Marine Science of the Gulf and Caribbean 7-(4) 10 pp.

Gulf of Mexico Its Origin, Waters, and Marine Life. Fishery Bulletin 89, Vol. 55, 1954, 601 pp.

Hovis, W. A., Forman, M. L., and Blaine, L.R., 1973: Detection of Ocean Color Changes from High Altitude, Goddard Space Flight Center Internal Technical Memorandum TMX-70559, 25 pp.

Jones, J. B., 1973: Determination of Chlorophyll Content of Water. Lockheed Electronics Corporation, Technical Memorandum DATM-061, Mississippi Test Facility, 7 pp.

Kemmerer, A. J., Benigno, J. A., Reese, G. B., and Minkler, F. C., 1973: A Summary of Selected Early Results from the ERTS-1 Menhaden Experiment, NASA CR-133152, 37 pp.

Knudsen, M., 1962: The Determination of Chlorinity by the Knudsen Method, Reprint by G. M. Manufacturing Company, 63 pp.

McClain, E. P. and Strong, A. E., 1969: On Anomalous Dark Patches In Satellite-Viewed Sunglint Areas, Monthly Weather Review, Vol. 97, No. 12, pp 875-884.

Ostle, B., 1963: Statistics in Research, Second edition, The Iowa State University Press, 585 pp.

Stevenson, W. H. and Pastula, E. J., Jr., 1973: Investigation Using Data from ERTS-1 to Develop and Implement Utilization of Living Marine Resources, Final Report, Mississippi Test Facility, Bay St. Louis, Mississippi, 185 pp.

Spiegel, M. R., 1961: Schaum's Outline of Theory and Problems of Statistics, McGraw-Hill, 359 pp.

Thomann, G. C., 1973: Remote Measurement of Salinity in an Estuarine Environment, Remote Sensing of Environment 2, 249 pp.

Weldon, J. W., 1973: Remote Measurement of Water Color in Coastal Waters, NASA Earth Resources Laboratory, Report 83, Mississippi Test Facility, 47 pp.

Wise, J. P. and Davis, C. W., 1973: Seasonal Distribution of Tunas and Billfishes in the Atlantic. NOAA Technical Report NMFS SSRF-662, 24 pp.

Woods, E. G. and Cook, P. C., 1973: Skylab Oceanic Gamefish Project. International Gamefish Research Conference, 73 pp.

Worthington, H. T., 1973: Remote Measurement of Surface Water Temperatures in Coastal Waters, NASA Earth Resources Laboratory, Report 85, Mississippi Test Facility, 33 pp.

Worthington, H. T., 1974: Personal Communication

Yentsch, C. S., 1960: The Influence of Phytoplankton on the Color of Sea Water, Deep-Sea Research, Vol. 7, p. 1.